ChemComm

COMMUNICATION

View Article Online
View Journal | View Issue

Cite this: *Chem. Commun.*, 2021, 57, 8360

Received 28th June 2021,
Accepted 27th July 2021

DOI: 10.1039/d1cc03437e

rsc.li/chemcomm

Benzene tricarboxamide derivatives with lipid and ethylene glycol chains self-assemble into distinct nanostructures driven by molecular packing†

Nada Aljuaid,[a] Mark Tully,[b] Jani Seitsonen,[c] Janne Ruokolainen[c] and Ian W. Hamley *[a]

The self-assembly in aqueous solution of benzene-1,3,5-tricarboxamide (BTA) bearing one alkyl chain and two PEG (polyethylene glycol) chains or two alkyl chains and one PEG chain yields completely distinct nanostructures. Two series of derivatives were synthesized and extensively characterized and electron microscopy and small-angle X-ray scattering (SAXS) reveal micelle structures for derivatives with one alkyl and two PEG chains, but nanotapes and nanoribbons for the series with two alkyl and one PEG chain.

Supramolecular polymerization is attracting great interest as a means to create innovative nanomaterials with unique properties stemming from the non-covalent self-assembly processes.[1] These can be either isodesmic self-assembly (equal association constants for the first and subsequent assembly steps) or nucleation/elongation or co-operative self-assembly.[2,3] Supramolecular polymerization is driven by a variety of intermolecular interactions including hydrogen bonding, π-stacking, metal–ligand interactions, hydrophobic or solvophobic interactions *etc.* It can occur in aqueous or non-aqueous solvents and the self-assembly process depends on these intermolecular interactions as well as solute–solvent interactions.[2]

Benzene-1,3,5-tricarboxamide (BTA) derivatives have recently been extensively studied by the groups of Meijer and Palmans[4,5] (as well as others) as model supramolecular polymers with a rigid π-stacking benzene motif surrounded by three hydrogen-bonding amide groups forming three-arm self-assembling molecules. BTA derivatives show promising properties as biomaterials,[6] organocatalysts,[7] stimuli-responsive materials,[8] among others, and as model systems to study supramolecular polymerization.[8,9]

In a recent paper, the self-assembly behavior was investigated for BTA derivatives in which two of the three arms are alkyl ethoxylates [12 methylene units connected to tetra(ethylene glycol)] and the third arm was a carboxylic acid with 1, 6 or 10 methylene units (or as a control a sample containing a tetra(ethylene glycol) carboxylate).[9] These molecules have hydrophobic chains around the benzene core and hydrophilic outer arm units. Nanostructures including fibers, membranes and nanotubes were observed *via* cryo-TEM and SAXS for the different BTA derivatives, depending also on concentration and temperature.[9]

In the present paper, we investigate for the first time the self-assembly in aqueous solution of BTA derivatives bearing simple combinations of one or two alkyl chains or ethylene glycols (oligo-ethylene glycols OEGs, or short polyethylene glycols, PEGs) as shown in Scheme 1. Table 1 summarizes the molecules synthesized. The alkyl chains were selected in the range C_{10} (decyl) to C_{18} (octadecyl), corresponding to the typical lengths of biological lipids which should provide self-assembly properties in molecules also bearing suitable short PEG chains, which were selected in the range $(EG)_4$ [tetra(ethylene glycol)] to $(EG)_{15}$. Sample names are of the form DAmMPEGn (m = number of carbon atoms in alkyl chain, n = number of ethylene glycol repeats) for the derivatives with two alkyl chains and a single

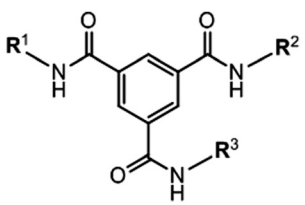

Scheme 1 Schematic of the scaffold of the BTA derivatives studied. Here R^1, R^2 and R^3 correspond to two PEG chains + one alkyl chain or two alkyl chains + one PEG chain as shown in Table 1.

[a] *Department of Chemistry, University of Reading, Whiteknights, Reading RG6 6AD, UK. E-mail: I.W.Hamley@reading.ac.uk*
[b] *ESRF-The European Synchrotron, 71 Avenue des Martyrs, Grenoble 38000, France*
[c] *Nanomicroscopy Center, Aalto University, Puumiehenkuja 2, Espoo FIN-02150, Finland*

† Electronic supplementary information (ESI) available: Experimental procedures including materials and methods, synthesis details and Schemes and characterization data (MS and NMR), UV and FTIR spectra and tables listing the parameters extracted from the fitting to the SAXS data. See DOI: 10.1039/d1cc03437e

Table 1 Molecules synthesized for which conformation and self-assembly were studied

(a) Derivatives with variable PEG chain length with C_{16} alkyl chain

	$(C_{16})_2PEG_n$	$C_{16}(PEG_n)_2$
PEG4	DA16MPEG4	MA16DPEG4
PEG8	DA16MPEG8	MA16DPEG8
PEG12	DA16MPEG12	MA16DPEG12
PEG15	DA16MPEG15	MA16DPEG15

(b) Derivatives with variable alkyl chain length with PEG12 chain(s)

	$(C_n)_2$PEG12	$C_n(PEG12)_2$
C_{10}	DA10MPEG12	MA10DPEG12
C_{12}	DA12MPEG12	MA12DPEG12
C_{16}	DA16MPEG12	MA16DPEG12
C_{18}	DA18MPEG12	MA18DPEG12

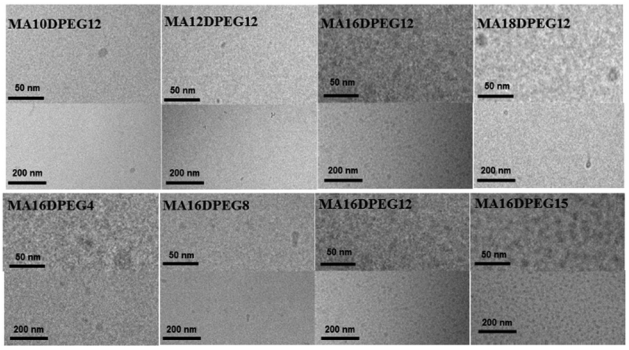

Fig. 1 Cryo-TEM images for the MAmDPEGn series (all 1 wt% aqueous solutions). For each sample, lower and higher magnification images are presented, to more clearly see the micelle structures.

PEG chain and MAmDPEGn for derivatives with one alkyl chain and two PEG chains (Table 1). All samples were found to be soluble at pH 3, 7 and 12. In the following, data is presented at native pH (approximately pH 7). We used a combination of cryo-TEM and SAXS to elucidate the self-assembled nanostructures in aqueous solution. Our results show distinct modes of self-assembly for BTA derivatives bearing one lipid chain and two PEG chains (if sufficiently short) compared to those with two PEG chains and one lipid chain.

Detailed schemes of the synthesis methods along with extensive characterization data are provided in the (ESI† Schemes S1–S4 and ESI† Fig. S1–S32). In brief, the DAmMPEGn BTA compounds were synthesized following the route reported by Meijer's group,[10] *i.e.* synthesis of 3,5-(methoxycarbonyl) isophthalic acid **3** (ESI† Scheme S1) through dihydrolysis of trimethyl benzene-1,3,5-tricarboxylate **2** followed by conversion to acyl chloride. The alkyl amine chain was reacted with acyl chloride forming a secondary amide in two positions. Methyl ester groups were used to protect the third position in compound **6** before reaction with PEGn amine followed the same procedure. This synthetic strategy used the desymmetrised BTA synthesis.[4,10] The MAmDPEGn compounds were prepared from benzene-1,3,5-tricarboxylic acid 1,3-dimethylester **8** (ESI† Scheme S2) through monohydrolysis of trimethyl benzene-1,3,5-tricarboxylate **2** before conversion to the acyl chloride by an acylation reaction. The alkyl amine chain was reacted with acyl chloride forming a secondary amide in one position. The methyl ester group in this case was used to protect the other two positions before the hydrolysis and acylation reaction with two equivalents of PEGn to produce compounds **12**.

Cryo-TEM was used to image nanostructures in aqueous solutions as it provides information on self-assembled structures, avoiding sample drying which occurs during sample preparation for conventional TEM and AFM. The images reveal that solutions of derivatives with mono-alkyl and di-PEG chains, *i.e.* MAmDPEGn form globular micelle-like structures in aqueous solution as shown in the cryo-TEM images in Fig. 1. The mono-alkyl derivatives with short alkyl chains (C_{10} or C_{12}) with DPEG12 do not show regular structures over the grid, these are only observed for longer alkyl chains (C_{16} in particular) where regular micelle structures with a defined diameter (*ca.* 6–8 nm) are observed extensively over the cryo-TEM grid (Fig. 1).

In complete contrast to the micelle structures formed by the MAmDPEGn series of samples, the micrographs for the DAmM-PEGn samples shown in Fig. 2 reveal the presence of extended tape-like structures when the alkyl chain is sufficiently long, with some differences in morphology from sample to sample. The two BTA derivatives with shorter alkyl chains, DA10M-PEG12 and DA12MPEG12 do not show a large population of self-assembled structures (only occasional structures were observed over the cryo-TEM sample grids, however nanostructures were detected by SAXS, *vide infra*). Solutions of DA18M-PEG12, DA16MPEG4, DA16MPEG8, and DA16MPEG12 all show nanotape morphologies in aqueous solution, with variation in nanotape width and curvature. Distinctly, DA16MPEG15 clearly self-assembles into remarkable twisted nanotape (nanoribbon) structures. However, all DAmMPEGn samples show the common feature that the self-assembled structures are based on planar 2-dimensional self-assemblies, a conclusion supported by detailed analysis of SAXS data discussed in the following.

The presence of intramolecular H–bonding was assessed by FTIR. IR spectroscopy shows vibrations for the N–H stretch at 3238 cm^{-1}, the C═O stretch at 1632 cm^{-1} and the amide II at 1564 cm^{-1} for DAmMPEGn (ESI† Scheme S31) which indicate the presence of intermolecular H–bonding. In contrast, the N–H stretch at 3344 cm^{-1}, the C═O stretch at 1651 cm^{-1} and the amide II peak at 1534 cm^{-1} for MAmDPEGn (ESI† Scheme S32) suggests the absence of threefold intermolecular H-bonds.

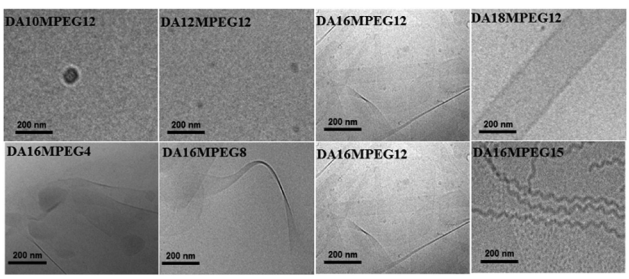

Fig. 2 Cryo-TEM images for the DAmMPEGn series (all 1 wt% aqueous solutions).

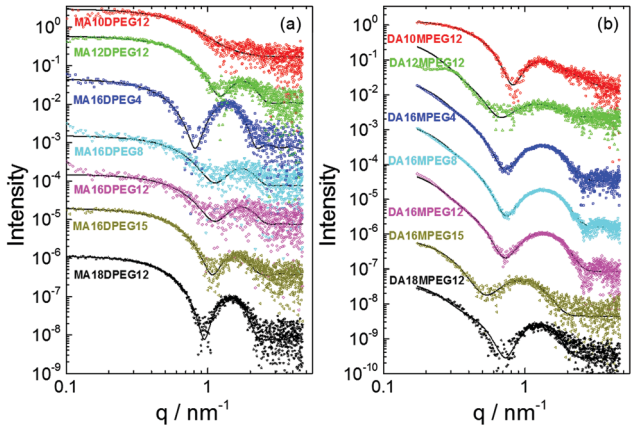

Fig. 3 Measured SAXS data (open symbols) and fitted form factors (models and fitted parameters listed in ESI† Tables S1 and S2). (a) MAmDPEGn series. (b) DAmMPEGn series. Data has been scaled to enable visualization.

This observation suggests that the lack of planar order in MAmDPEGn may be influenced by the absence of H–bonding molecular interactions.

SAXS is a powerful method to probe self-assembled nanostructures *in situ*[11] and was applied to quantitatively determine the form factors and hence dimensions and scattering (electron density) contrasts of the assemblies formed by the BTA derivatives. The measured data along with form factor fits are presented in Fig. 3. The SAXS profiles in Fig. 3a show that all MAmDPEGn samples form micelles to a certain extent, except MA10DPEG12 which shows features of a monomeric form factor (data fitted using a generalized Gaussian coil form factor model, allowing for swelling or collapse *via* a variable Flory exponent in the radius of gyration). SAXS is able to detect micelle formation for some samples for which only a low population of micelles was observed by cryo-TEM. The parameters from the fitted spherical core–shell particle form factor are listed in ESI† Table S1. These show that the outer radius lies in the range 3.1–3.8 nm, which is both consistent with the cryo-TEM images in Fig. 1 and physically realistic, considering estimations of the length of the molecules, for example for MA16DPEG15, the extended alkyl chain length is approximately 1.8 nm and the PEG radius of gyration is about 1.5 nm. The obtained inner core radii values listed in ESI† Table S1 are actually slightly lower than the extended alkyl chain lengths, which may indicate folding, however in addition the boundaries between core and shell will be diffuse and it also has to be considered that the BTA residues must presumably reside at the outer part of the core. No general significant trends in the core or shell radius were observed across the samples, the values reflecting the length of both hydrophobic and hydrophilic chains and the balance of these that affects the core–shell interfacial area and hence molecular packing. This is also influenced of course by the positioning of the BTA residues at the interface between the inner lipid-rich core and the outer PEG corona.

The SAXS data in Fig. 3b for DAmMPEGn solutions have a different scaling at low wavenumber q and shape of form factor maxima, indicating distinct nanostructures to those for the MAmDPEGn samples. Motivated by these features and the presence of nanotape structures in the cryo-TEM images (Fig. 2), the SAXS data were fitted to form factors of bilayer structures (some samples gave weak SAXS profiles indicating low populations of the nanostructures imaged by cryo-TEM). This form factor fits the data very well. The model is based on that used for lipid bilayers[12] and represents the electron density profile across the bilayer as a sum of three Gaussian functions, one representing the hydrocarbon centre of the bilayer (with a negative electron density relative to the solvent) and the other two (positive electron density contrast) Gaussians symmetrically representing the outer surfaces. SAXS is able to accurately determine the layer thickness, which cannot reliably be obtained from the cryo-TEM images. The fit parameters are detailed in ESI† Table S2. The results indicate that the chains in the bilayer are highly interdigitated, since the layer thicknesses are less than twice the estimated extended length of the alkyl chains, for example for C_{18} chains, the chain length is approximately 2.0 nm whereas the layer thickness t = 2.47 nm according to the SAXS form factor fitting for DA18MPEG12 (ESI† Table S2) and in addition the PEG chain outer layers will have finite thickness (*ca.* 0.97 nm radius of gyration assuming Gaussian coil conformation).

Based on the results from cryo-TEM and SAXS, we propose the model shown in Fig. 4, which is consistent with simple molecular packing argument, *i.e.* applying the surfactant packing parameter model[13–15] to the case of the BTA derivatives which have a highly constrained tri-functional linking unit compared to conventional amphiphiles. Samples MAmDPEGn with mono-alkyl chains of sufficient length and two PEG chains form micelle structures due to packing constraints of the hydrophilic di-PEG headgroup and hydrophobic mono-alkyl core group (Fig. 4). In the surfactant packing parameter description, the molecules would be considered to have a cone-like shape. In contrast, the samples with di-alkyl chains of sufficient length (and appropriate single PEG chains) pack into nanotape structures based on layered stacking of the BTA

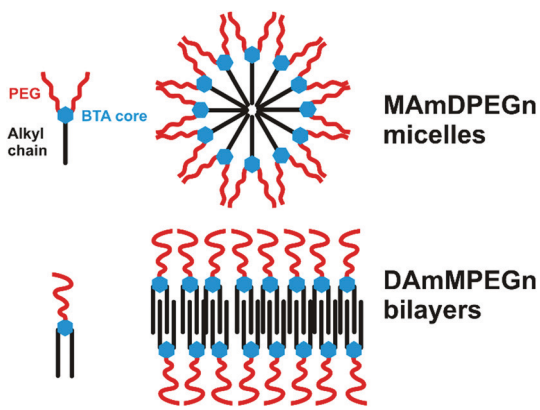

Fig. 4 Proposed models for self-assembly. Top: MAmDPEGn series with mono-alkyl chain and di-PEG, Bottom: DAmMPEGn series with di-alkyl chains and mono-PEG.

derivatives into bilayers with a core of hydrophobic di-alkyl chains coated by hydrophilic PEG, here there is less drive towards curvature at the interface, the molecules pack as effective cylinder-shaped objects.[13,14]

The possible presence of micelles in certain BTA derivatives has been suggested in several reports,[16,17] but to the best of our knowledge we provide the first direct evidence for such structures in the novel BTA derivatives investigated. Nanosheets have been observed in BTA derivatives with a hydrophobic core linked to outer oligoethylene glycol units on two chains (the other arm bearing lipidic carboxylic acids).[9] Micelle and nanotape structures have been observed for lipopeptide systems[1,18–20] and studies have explored the effect of the number of alkyl chains on the self-assembly which includes an example where micelle and nanotape structures are observed depending on the number of palmitoyl (C_{16}) chains.[21] Nanotape structures are rarely observed for lipids themselves, which tend to form lamellar assemblies (or micelles) depending on concentration *etc.*, and neither are they commonly reported for mixed arm block polymers in selective solvents, for which however micelles and vesicles have been observed.[22–25]

In summary, we show that control of the self-assembled nanostructure of BTA derivatives in aqueous solution can be achieved by balancing the number and length of attached hydrophilic and hydrophobic chains. BTA derivatives have provided an exceptional platform for model studies of self-assembling systems, especially one-dimensional self-assembly.[1,8,26,27] Here, we present evidence that novel BTA derivatives undergo self-assembly into zero- and two-dimensional structures. This will be valuable for future fundamental studies of self-assembly (nucleation, kinetics, self- and cross-seeding *etc.*) as well as potential applications as delivery agents, viscosity modifiers and many others and also as platforms for further functionalization.

N. A. acknowledges support from the Saudi Arabian Cultural Bureau. IWH was supported by EPSRC Platform grant EP/L020599/1. We thank the ESRF for the award of beam time (ref. MX-2345). We are grateful to Dr Lewis Hart for advice concerning synthesis.

Conflicts of interest

There are no conflicts to declare.

Notes and references

1 T. Aida, E. W. Meijer and S. I. Stupp, *Science*, 2012, **335**, 813–817.
2 M. F. J. Mabesoone, A. R. A. Palmans and E. W. Meijer, *J. Am. Chem. Soc.*, 2020, **142**, 19781–19798.
3 M. A. J. Veld, D. Haveman, A. R. A. Palmans and E. W. Meijer, *Soft Matter*, 2011, **7**, 524–531.
4 S. Cantekin, T. F. A. de Greef and A. R. A. Palmans, *Chem. Soc. Rev.*, 2012, **41**, 6125–6137.
5 C. Kulkarni, E. W. Meijer and A. R. A. Palmans, *Acc. Chem. Res.*, 2017, **50**, 1928–1936.
6 S. Varela-Aramburu, G. Morgese, L. Su, S. M. C. Schoenmakers, M. Perrone, L. Leanza, C. Perego, G. M. Pavan, A. R. A. Palmans and E. W. Meijer, *Biomacromolecules*, 2020, **21**, 4105–4115.
7 L. N. Neumann, M. B. Baker, C. M. A. Leenders, I. K. Voets, R. P. M. Lafleur, A. R. A. Palmans and E. W. Meijer, *Org. Biomol. Chem.*, 2015, **13**, 7711–7719.
8 G. Vantomme, G. M. ter Huurne, C. Kulkarni, H. M. M. ten Eikelder, A. J. Markvoort, A. R. A. Palmans and E. W. Meijer, *J. Am. Chem. Soc.*, 2019, **141**, 18278–18285.
9 N. M. Matsumoto, R. P. M. Lafleur, X. W. Lou, K. C. Shih, S. P. W. Wijnands, C. Guibert, J. van Rosendaal, I. K. Voets, A. R. A. Palmans, Y. Lin and E. W. Meijer, *J. Am. Chem. Soc.*, 2018, **140**, 13308–13316.
10 J. Roosma, T. Mes, P. Leclere, A. R. A. Palmans and E. W. Meijer, *J. Am. Chem. Soc.*, 2008, **130**, 1120–1121.
11 I. W. Hamley, *Small-Angle Scattering: Theory, Instrumentation, Data and Applications*, Wiley, Chichester, 2021.
12 G. Pabst, M. Rappolt, H. Amenitsch and P. Laggner, *Phys. Rev. E: Stat. Phys., Plasmas, Fluids, Relat. Interdiscip. Top.*, 2000, **62**, 4000–4009.
13 J. N. Israelachvili, D. J. Mitchell and B. W. Ninham, *J. Chem. Soc., Faraday Trans. 2*, 1976, **72**, 1525–1568.
14 J. N. Israelachvili, *Intermolecular and Surface Forces*, Academic Press, San Diego, 1991.
15 I. W. Hamley, *Introduction to Soft Matter. Revised Edition*, Wiley, Chichester, 2007.
16 L. Albertazzi, F. J. Martinez-Veracoechea, C. M. A. Leenders, I. K. Voets, D. Frenkel and E. W. Meijer, *Proc. Natl. Acad. Sci. U. S. A.*, 2013, **110**, 12203–12208.
17 X. Lou, R. P. M. Lafleur, C. M. A. Leenders, S. M. C. Schoenmakers, N. M. Matsumoto, M. B. Baker, J. L. J. Van Dongen, A. R. A. Palmans and E. W. Meijer, *Nat. Commun.*, 2017, **8**, 8.
18 H. G. Cui, M. J. Webber and S. I. Stupp, *Biopolymers*, 2010, **94**, 1–18.
19 I. W. Hamley, *Soft Matter*, 2011, **7**, 4122–4138.
20 I. W. Hamley, *Chem. Commun.*, 2015, **51**, 8574–8583.
21 I. W. Hamley, S. Kirkham, A. Dehsorkhi, V. Castelletto, M. Reza and J. Ruokolainen, *Chem. Commun.*, 2014, **50**, 15948–15951.
22 Z. Li, M. A. Hillmyer and T. P. Lodge, *Langmuir*, 2006, **22**, 9409–9417.
23 I. W. Hamley, *Block Copolymers in Solution*, Wiley, Chichester, 2005.
24 A. O. Moughton, M. A. Hillmyer and T. P. Lodge, *Macromolecules*, 2012, **45**, 2–19.
25 A. H. Groschel and A. H. E. Muller, *Nanoscale*, 2015, **7**, 11841–11876.
26 J. van Gestel, A. R. A. Palmans, B. Titulaer, J. Vekemans and E. W. Meijer, *J. Am. Chem. Soc.*, 2005, **127**, 5490–5494.
27 C. M. A. Leenders, L. Albertazzi, T. Mes, M. M. E. Koenigs, A. R. A. Palmans and E. W. Meijer, *Chem. Commun.*, 2013, **49**, 1963–1965.